Dissolved organic matter controls of arsenic bioavailability to bacteria

Martin Pothier, Véronique Lenoble, Cédric Garnier, Benjamin Misson, Charlotte Rentmeister, Alexandre Poulain

Dissolved organic matter controls of arsenic bioavailability to bacteria

Martin P. Pothier[a], Véronique Lenoble[b], Cédric Garnier[b,c], Benjamin Misson[b], Charlotte Rentmeister[a], Alexandre J. Poulain[a,*]

[a] *Biology Department, University of Ottawa, 30 Marie Curie, Ottawa, ON, K1N 6N5, Canada*

[b] *Univ. Toulon, Aix Marseille Univ., CNRS/INSU, IRD, MIO UM 110, Mediterranean Institute of Oceanography, La Garde, France*

[c] *Deceased*

* Corresponding author email : apoulain@uottawa.ca

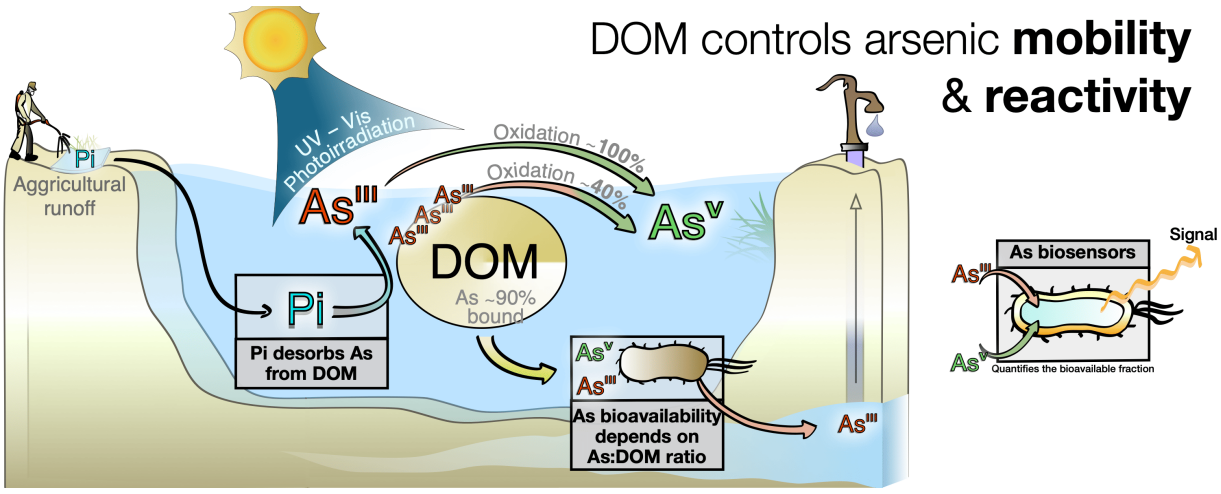

Graphical abstract

ABSTRACT

The presence of arsenic in irrigation and drinking waters is a threat to worldwide human health. Dissolved organic matter (DOM) is a ubiquitous and photoreactive sorbent of arsenic, capable of both suppressing and enhancing its mobility. Microbes can control the mobilization of mineral-bound arsenic, through redox processes thought to occur intracellularly. The role that DOM plays on the bioavailability of arsenic to microbes is often invoked but remains untested experimentally. Here, using a whole-cell biosensor, we tested the role of DOM on As (III) and As(V) bioavailability. Using cation amendments, we explored the nature of As-DOM interactions. We found As bioavailability to be dependent on [As]/[DOM] ratio and on the strength of As binding to DOM which varied as a function of time. We further tested the role of DOM on As(III) photooxidation and showed that As (III) photooxidation rate is limited by the strength of its interactions with DOM and sensitive to ionic competitive desorption. Our study demonstrates the dynamic control that photoreactive DOM poses on the bioavailability and reactivity of As in the environment and highlights the kinetic controls that DOM can possibly exert on As toxicity at various levels in foodwebs.

Keywords: biosensor; bioavailability; arsenic; water quality; photooxidation

Arsenic (As), classified as a group 1 carcinogen (*1*), is estimated to affect the food and drinking waters of over 140 million people worldwide (*2*). The effects of human-mediated As release through mining, farming and manufacturing processes (*1, 3*) are observed at local, or even regional scales (*3*). Microbes, ubiquitous organisms operating at a global scale (*4*), are capable of affecting As mobility via catabolic (e.g. *aio, aso, aox, arr…*) or resistance (e.g. *ars, arsM…*) pathways (*5, 6*). Therefore, conditions limiting As availability to microbes will reduce As remobilization.

Several environmental drivers of As bioavailability have been proposed (*7*) but very few have been directly tested. Such drivers include changes in redox (*8*), nutrients (*9*), cations (*10*) and solar radiation, known to profoundly affect organic material degradation, nutrient release and organic matter mineralization (*11*). Recently, Langner *et al.* (*12*) have presented spectroscopic evidence of covalent bonds between trivalent arsenic (As(III)) and natural organic matter (NOM) suggesting that NOM strongly governs the bioavailability and thus the mobility of As in anoxic peat.

DOM acts as a ubiquitous environmental sorbent of As through the formation of covalent (*12*) and ternary complexes with As (*13, 14*), thereby preventing solid phase sorption (*7*) and maintaining high As levels in soils (*15*) and in water (*16-18*). With the rise of terrestrially-derived DOM concentration of surface waters over the past few decades (*19*), we can expect that the role that DOM plays on As cycling will be increasing. The current mechanistic understanding of the interactions between As species and DOM includes: i) specific binding of As(III) to sulfur (*12*), and to amino (*20*) functional groups within DOM; ii) indirect cationic bridging of As(V) with calcium (*14*) and of As(III) with iron (*21*), and iii) weak electrostatic complex formation of As(III) and As(V) with phenolate or carboxylic functional groups (*13, 21*). Furthermore, previous experiments during which we evaluated As bioavailability in 17 lakes sampled around Giant Mine (YK, Canada) and exhibiting a wide range of As and DOC concentrations, identified a role for DOC on As bioavailability (*22*). Surprisingly, we found that newly added As to lake water samples was less

bioavailable than older, "legacy" arsenic, already present in the system. This led us to hypothesize that As-DOM complex aging is important in controlling its bioavailability.

In this study, we hypothesized that DOM acts as a strong predictor of As bioavailability to microbes and predicted that strong As binding to DOM would reduce the pool of As available for microbial uptake. Using an As-specific biosensor (*22*), we monitored for changes in As(III) and As(V) bioavailability by altering [As]/[DOM], equilibration time, DOM origin, and investigated the role of DOM photoirradiation on As redox state and bioavailability. We found As bioavailability to be dependent on [As]/[DOM] ratio and on the strength of As binding to DOM which varied as a function of time.

1. MATERIALS AND METHODS

1.1. Reagents

All media and reagents were made and kept in pre-sterilized, acid washed containers. Purification of ultrapure water (Milli-Q), preparation/preservation of the 10 mM As standards, and constituents of growth (LB & MGP) and exposure media (MGP & MIP) have been previously described (*22*). Dissolved organic matter (DOM) standards were sourced from the International Humic Substance Society (IHSS): i) Suwannee River Natural Organic Matter 2R101N (NOM), ii) Suwannee River Humic Acid 3S101H (SRHA), iii) Suwannee River Fulvic Acid 3S101F (SRFA), and iv) Elliott Soil Fulvic Acid 5S102F (ESFA). These represented a wide-range in sulfur (0.41 to 1.78% (w/w)), carboxyl (9.13 to 13.24 $mg \bullet g^{-1}$ C) and phenolic (2.27 to 3.72 $mg \bullet g^{-1}$ C) functional groups (*23-25*). Properties of the DOM origins used to produce this RDA can be found in Supplementary Information (Supplementary Table). DOM standards were prepared in acid washed volumetric flasks at 100 $mg \cdot L^{-1}$ by dissolving 0.0050 g in 50 mL of ultra-pure (Milli-Q) water and incubated at 37 °C and 200 RPM for 24 h. Orbital

shaking/incubation ensured complete dissolution of the standards in Milli-Q water without adjustment of ionic strength or pH. Filtropur 0.2 µm PES membranes filters (Sarstedt 83.1826.001) were used to ensure sterility of the standards and prevent microbial degradation during storage. Refraining from using buffering and preservation agents drove the pH to approximately 4.5. All DOM standards were prepared following the above noted method, and kept in dark containers at 4 °C for no longer than 3 weeks.

1.2. Containers

Containers used in this study include: i) Simport Scientific polypropylene 3 mL containers (Fisher Scientific 22-040-408) for all DOM incubation treatments that did not involve photoirradiation; ii) Globe Scientific Spectrophotometer polymethyl methacrylate 4.5 mL UV grade (280–800 nm) cuvettes (Fisher Scientific 111157) for all photoreactor assays; iii) Nalgene® High Density Polyethylene (HDPE) 500 mL bottles for all dialysis experiments, and Trace Metal Grade Corning® tubes for storage and analyses; and iv) Fisherbrand glass bottles (FB800100) for all media and reagent storage.

1.3. Biosensor Culture and Exposure Protocol

Biosensor construct, speciation protocol, and instrumentation used to incubate and quantify fluorescent output and culture yield of the biosensors are fully described elsewhere (*22*). Briefly, the biosensing construct was inspired by the design of J. Stocker (*26*), for which we used two ArsR binding sites shown to provide optimal detection while minimizing noise. The sensing-reporting sequence (ArsRBS2-mCherry) was constructed by custom gene synthesis (Integrated DNA Technologies) and cloned into the XmaI and XbaI restriction sites of the high copy pUCP19 shuttle vector upstream of the sequence encoding for mCherry. The reporter plasmid was transformed into *E. coli* NEB10-beta (New England BioLabs) – a level 1, non-pathogenic, non-regulated host. The MGP growth and exposure media, comprised of glycerol and organic phosphate, were used in all biosensor exposure assays. Use of

these media was found to allow for the uptake of over 94% of the added As(III) and As(V) additions (*22*).

For all assays, As concentration was set at 200 nM because this concentration falls at a mid-point in the linear range of the biosensor's calibration curve and has previously led to reproducible quantification (*22*). Furthermore, this concentration is environmentally relevant as the World Health Organization set a guideline of 133 nM (10 µg/L) for As in drinking water (*27*). Biosensor exposure protocol consists of two steps. First, all working solutions (DOM, ions, and As) were prepared at a final concentration of 2× and added to the containers in the following order: (i) Milli-Q water, (ii) DOM, (iii) cations (if required), and (iv) arsenic. Time of interaction prior to exposing the biosensor cells was assay dependent and conducted in the dark and at room temperature. Second, pre-incubated working solutions were then subsampled into three separate wells on the 96 well plate then analyzed by three individually grown biosensor cultures. Exposure occurred in the following order: (i) 100 µL subsample of the pre-incubated 2× concentrated working solution, (ii) 80 µL of 2× concentrated exposure medium (MGP or MIP), and (iii) 20 µL of MGP grown biosensor cells for a final biosensor cell concentration of 10%.

1.4. Data analysis

The biosensor fluorescent output present in all figures has been corrected for autofluorescence, noise and culture health using R programming language. First, autofluorescence is a background interference that differs by DOM origins, bacteria cultures, reagents, and by well in the exposure plate. Standardization consists of subtracting endpoint output signal (20 h) of each well from the initial output (T0) of that same well (**Fig. S7**a). Second, we refer to background noise as the signal produced by biosensor cells that are not exposed to As; even in the absence of the inducer (As) there is a basal expression of fluorescence that must be controlled for. Removal of background noise consists of the difference between signal output of the treatment (e.g. As + SRHA) and of the no-As control at the same timepoint (20 h)

and of the same biosensor culture (**Fig. S7**b). Third, differences in biosensor fitness or yield can arise when working with environmental samples (**Fig. S1**). Normalization consists of dividing the corrected output signal by the culture's optical density (OD600) at the same time point (**Fig. S7**c). Finally, assuming no-DOM controls represents 100% bioavailability, we can convert the biosensor's fluorescent output signal to percent biouptake. This correction involves dividing the normalized biosensor output of the treatments (e.g. As + SRHA) by output signal of the As-only calibration point control and multiply by 100 (**Fig. S7**d).

1.5. Photoirradiation

A Luzchem Photoreactor was used for all photoirradiation assays. These consisted of a 22 h pre-incubation assay followed by a 4 h irradiation step subsampled at 0 h (T0), 2 h (T2) and 4 h (T4). Similarly to the exposure protocol previously described, samples were prepared, incubated, and irradiated at 2× their final concentration (400 nM As(III) & 20 mg/L DOM), then diluted to 1× upon exposure to the biosensors. The power per unit area (irradiance) for wide-band UV radiation was measured using GOLDILUX ultraviolet meters, UVA (315–400 nm), and UVB spectrum (280–315 nm). Irradiance intensity for UVA averaged 0.037 $J \bullet m^{-2} \bullet s^{-1}$ and for UVB averaged 0.129 $J \bullet m^{-2} \bullet s^{-1}$. Spectral components of light from 200 nm to 1000 nm were analysed using a ThorLabs compact CCS200 (**Fig. S5**).

1.6. Chemical analysis

Cross-analysis of HPLC-ICP-MS and the biosensor speciation technique was performed on the same-day and on the same samples. Subsamples for As speciation analysis were preserved using HNO_3 at 0.3% (2 µL of 70% HNO_3 in 398 µL Milli-Q plus 100 µL of sample). Details regarding HPLC-ICP-MS speciation analysis are detailed elsewhere (*22*).

1.7. Dialyses experiments

All dialysis experiments, used to quantify the fraction of As bound to DOM, were performed in triplicate and consisted of adding DOM (10 mg•L^{-1}) and As (200 nM, either As(III) or As(V)) to the inside of a dialysis bag (pore size 500 Da). Similarly to the biosensor exposure assays, no buffering agents were used. For experiments involving major ions, 10 mM Na^{+} or Ca^{2+} were added both inside the dialysis bag and in the external solution, at the same ionic strength to prevent crossing of As induced by osmotic gradient. Quantification of As species levels (ICP-MS) for the external solution, was performed at both T0 and T24 h whereas measurement for the internal solution was only quantified after a 24 h contact time. Here, quantification of [As] inside the dialysis bag represents both bound and unbound As, whereas quantification of the outside fraction represents only the "free" or unbound fraction. All concentrations in µg•L^{-1} used to determine the bound fraction were first converted to pmols to account for differences between internal (3 mL) and external (300 mL) volumes before percent conversions (**Fig. S3**).

1.8. FEEM analysis

Measurement of Fluorescence Excitation/Emission Matrices (FEEM), were performed in triplicate by mixing DOM (10 mg•L^{-1}) and As (200 nM, either As(III) or As(V)) to a 3 mL quartz Suprasil cells, at room temperature, in the dark. No buffering or acidifying agents were used. Fluorescence Excitation/Emission Matrices were regularly measured on a HITACHI F4500 spectrofluorometer. The excitation wavelength ranged from 320 to 460 nm, with 10 nm step and an excitation slit of 1 nm. The corresponding emission spectra were acquired from 350 to 550 nm with a scan speed of 2400 nm•min^{-1} and a slit of 1 nm. The photomultiplier tension was fixed at 950 V and the integration time set at 0.1 s. The extraction of the 5 nm

193 stepped emission was obtained by FL-Solution software. Each experiment was
194 performed in triplicate.

195

196 ## 2. RESULTS AND DISCUSSION

197 ### 2.1. DOM kinetically controls As bioavailability to bacteria

198 In a first series of experiments, we tested the role of i) DOM concentrations and ii)
199 the duration of As-DOM pre-incubation, prior to exposure to the biosensor, on the
200 bioavailability of As(III) and As(V). Here, DOM was provided as Suwannee River
201 Humic Acid from IHSS over a range of concentrations representative of what can
202 typically be found in natural surface waters (streams, lakes, wetlands) and
203 porewaters (*28*).

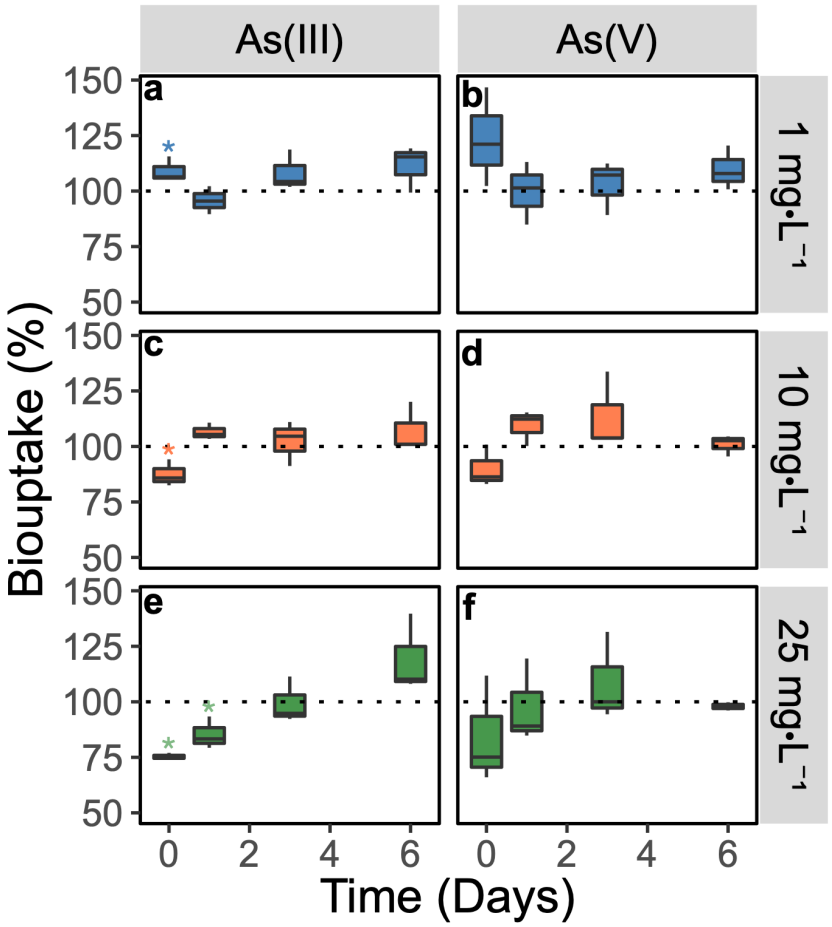

Fig. 1 | DOM control on As(III) and As(V) bioavailability over time. DOM control on As(III) and As(V) bioavailability over time. Boxplots represent biological replicates (n = 3) containing either 200 nM of As(III) (a, c, e) or 200 nM As (V) (b, d, f) in the presence of a DOM (SRHA) gradient (vertical facets). Axes include room-temperature pre-incubation time (X-axis) and output signals of treatments are indicated as percent deviation from our no-DOM controls (Y-axis). Dotted line represents biosensor output signal of the no-DOM controls. Stars represent a significant decrease from the 200 nM (no-DOM) control incubated for the same period of time determined using raw fluorescent signals and TukeyHSD post-hoc analysis on a oneway ANOVA.

First, we observed that without a pre-incubation step, addition of 25 mg/L SRHA decreased As(III) and As(V) bioavailability by 25% and 16%, respectively (significant decrease of 25% for As(III), $p<0.0001$) (**Fig. 1**e), supporting our previous observation with natural lake water samples (*22*). Second, in the presence of [SRHA] ≥ 10 mg•L^{-1}, As(III) and As(V) bioavailability increased with increasing pre-incubation time (**Fig. 1**e), to values comparable to the no-DOM control (**Fig. 1**c-f). Here, the pre-incubation time required to reach control values ranged from 1 ([SRHA] = 10 mg•L^{-1}) to 3 days ([SRHA] = 25 mg•L^{-1}). After a 6 day pre-incubation time in

the presence of [SRHA] = 25 mg•L^{-1}, As(III) bioavailability was greater than in the no-DOM control. This corresponded to a significant increase of 45% of As bioavailability over a 6-day period ($p<0.001$). Note that increasing DOM concentration also stimulated biosensor cells yield (**Fig. S1**c-f), probably due to the presence of nutrients within the DOM pool but this stimulation was not time dependent and did not affect accuracy of the As-specific biosensor signal (**Fig. 1**c-f).

Our data showed that DOM hampered As bioavailability at low As (III) to DOM ratio (8 nmol As(III) • mg^{-1} DOM) and during a short time period after As and DOM were placed together ($t < 30$ min). This observation is in line with what was predicted in the literature. Indeed, both higher stability constants (*29*) and stronger binding (*21*) have been reported when working at pH and [As]/[DOM] ratios similar to the values used in this study. Using a two-site ligand binding model, Liu and Cai (2010) have shown that humic acids have a limited number of strong As binding sites that are sensitive to increases in [DOM] (*29*). Furthermore, Bushmann *et al.* (*21*) proposed that the limited number of strong As binding sites on DOM is sensitive to competition and/or conformational changes of humic macromolecules, which may explain the time-dependent nature of our results.

To document a possible change in DOM conformational properties over time and in the presence of As, we used FEEM (Fluorescence Excitation/Emission Matrices). Though widely used to quantify DOM, contour maps of the 3D FEEM can also be used to characterize changes in DOM's fluorescent components (*30*). Using FEEM, we predicted that time-dependent changes in fluorescence would correspond to changes in the nature of the interactions between As and DOM. Using colour distance matrix and k-mean cluster analyses, we confirmed a change in fluorescence spectrum intensity and profile over time, both peaking in intensity after a 2-day incubation and shifting in profile following a 6-day incubation (**Fig. S2**). Changes in the molecular conformation of DOM over time can result from modifications of the surface charge (*31*), and from the intramolecular cationic bridging (*32*). We recognize that

fluorescence data presented here offer little mechanistic insights into the underlying interactions between As and DOM. That being said, quantification of changes in fluorophore intensity (or quenching) through time does present evidence of the dynamic nature of As-DOM interactions (**Fig. S2**), which is also reflected in the response of the biosensor (**Fig. 1**).

It is generally recognized that cationic metal-DOM interactions strengthen over time. Arsenic, an oxyanion under most environmentally relevant conditions, would predictably offer different binding dynamics. We propose that increasing As(III) bioavailability over time resulted from a series of ligand exchange within the DOM pool, induced by DOM conformational changes; this transfer of As(III) from the few sites at which it formed strong bonds, towards sites that are more abundant but exhibiting weaker electrostatic affinity, made it more accessible to the biosensor and hence bioavailable. Contrary to what appears to be currently accepted in the literature for bacteria (*33*) and derived from DGT experiments (*34*), our data suggest that inorganic As species do remain bioavailable in the presence of DOM, through time, even when abiotic conditions favour As complexation.

In addition to free As species, As weakly bound to DOM also represents a pool of labile As that is bioavailable to microbes. Furthermore, microbial cells themselves may play a role in actively releasing weakly-bound As from DOM. Possible mechanisms include: i) internalization of co-transported As during microbial consumption of DOM (*35*); ii) release of weakly-bound As induced by extracellular electron transfer (*36*) and shuttled by quinone moieties within the DOM pool (*37, 38*); and iii) uptake of As through siderophores channels (e.g. ABC-type exporters (*39*)) that are possibly upregulated by phosphate/iron starvation during biosensor growth. Determining the mechanisms involved will require further work.

2.2. The nature of As binding to DOM controls its bioavailability

Our interest in identifying the mechanism involved in DOM's control on As bioavailability required more targeted experiments. Carboxylic groups are one of the main contributors to DOM's negative charge (*40*) and thus promote strong surface and inner-sphere complexes with cationic metals (*21, 41, 42*). Moreover, cations are known to affect the sorption of As to DOM by changing its affinity to functional moieties such as carboxylic, phenolic, amino and sulfhydryl groups (*12, 21, 29*). These associations can induce aggregation and structural re-orientation of the organic matter by increasing the compression and rigidity of the structure while favoring a hydrophobic core (*43*).

We first tested the effect of cations on As bioavailability in the presence of DOM (20 nmol As•mg^{-1} DOM), by adding 10 mM Na^+, 10 mM Ca^{2+}, or 5 µM Cu^{2+}. Mono- and di-valent cations (Na^+ and Ca^{2+}) were selected for their ubiquity in the environment and pronounced effects on DOM charge (*44*) and structure (*45*), respectively. Cu^{2+} is a trace metal with high affinity for DOM (*46*), and is expected to form strong covalent bonds at complexation sites (*47, 48*). The concentration of cations was limited by their toxicities and chosen to maintain relevance to concentrations commonly found in freshwaters. We found that across all tested commercially available DOM treatments, As(III) and As(V) bioavailability variably increased in the presence of Cu^{2+}, was unaffected in the presence of Na^+, and consistently decreased in the presence of Ca^{2+} (**Fig. 2**). These data suggest that the mechanisms involved in controlling As bioavailability are conserved across DOM samples.

Experiments performed in the presence of copper support our finding that strong binding of As to DOM limits its bioavailability. In this case, we suspect that the presence of Cu^{2+} prevented As binding, maintaining its accessibility and bioavailability to the biosensor. Although the mechanism remains unclear, we speculate that it relates to the nature of the DOM conformational changes differentially induced by calcium and copper. Copper, like calcium, electrostatically interacts with

303 deprotonated carboxylic groups of DOM (*46, 49*). Copper (*49*), like calcium,
304 electrostatically interacts with deprotonated carboxylic groups of DOM (*46*).
305 However, Ca^{2+} interactions with DOM differ from that of copper in the strength and
306 specificity of the bonds it forms with DOM (*46, 49*). Indeed, calcium is thought to
307 better penetrate DOM structure (*50*), thereby forming strong inner-sphere ionic
308 bridges (*14, 42, 50*), creating more space for water molecules (*51*), and changes in
309 DOM conformation (*43, 52*).

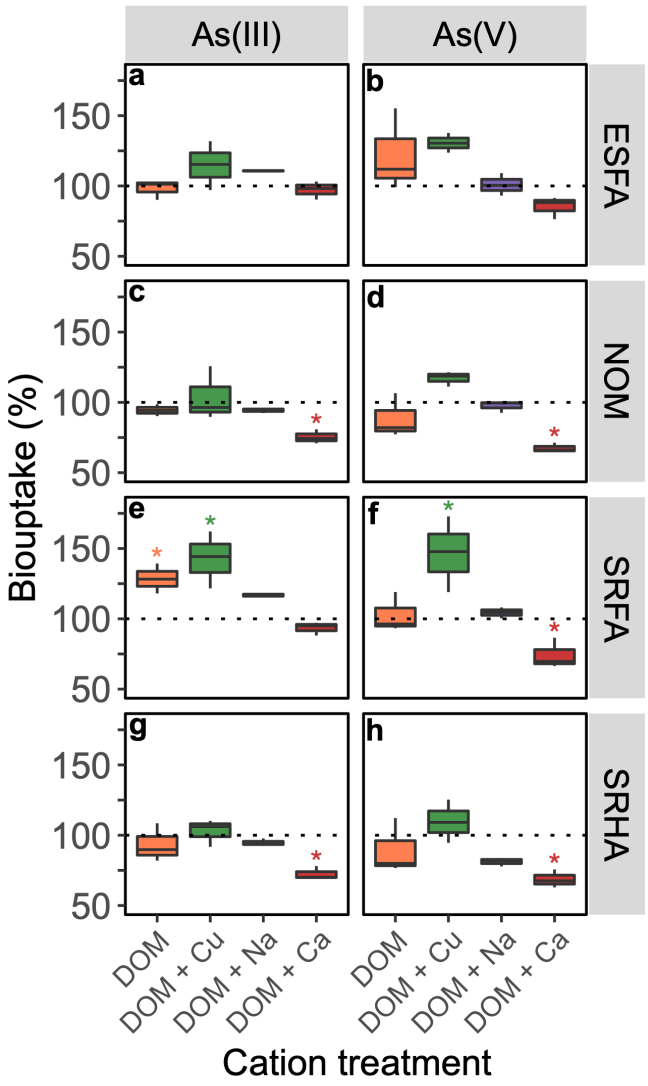

Fig. 2 | As bioavailability in the presence of DOM of varying origins. Changes in As bioavailability (Y-axis) were plotted over various cation treatments (X-axis). Environmentally relevant concentrations of Na^{+} (10 mM), Ca^{2+} (10 mM), Cu^{2+} (5 μM), and DOM (10 mg•L^{-1}) were used. The origin of the DOM used is identified by the vertical facet labels. Each box represents the mean and standard deviation of biological triplicate samples containing 200 nM of As(III) (a, c, e, g) or 200 nM As(V) (b, d, f, h). Percent conversions were based on presence vs absence of organic matter. Dotted line represents biosensor output signal of the no-DOM controls at the same ionic strength. Significant decrease from the no-DOM controls were determined using TukeyHSD post-hoc analysis on a one-way ANOVA.

Second, to test the extent to which As(V) binding to DOM affected its bioavailability, we subjected the exposure solution to a 500 Da dialysis membrane bag in the presence and absence of SRHA, Ca^{2+} or Na^{+}. In the absence of cations, >95% of As(V) was bound to SRHA, yet remained bioavailable (**Fig. S3**). Although the addition of Na^{+} and Ca^{2+} decreased the extent to which As(V) was bound to DOM (**Fig. S3**),

only in the presence of Ca^{2+} did we observe a 25% decrease in the bioavailability of As bound to DOM (**Fig. 2**). These results confirm that microbes are not limited to the unbound fraction of As but are also be capable of accessing weak electrostatically held As.

We used FEEM to test the effects of Na^{+} and Ca^{2+} amendments on As(V)-SRHA treatments (**Fig. S4**). Both colour distance matrix and k-mean cluster analysis confirmed that all three Ca^{2+} treatments increased fluorescence intensity beyond that of the Na^{+} treatments and of the no-cation controls, suggesting an important role of Ca^{2+} in changing the structural properties of DOM. These findings are in line with reports indicating that Ca^{2+} affects DOM structure, namely its compression and rigidity (*43, 52*). Following the two-site ligand binding model proposed by Buschmann et al. (2006) and further characterized by Liu and Cai (2010), it is conceivable that changes to the molecular structure and arrangement of DOM evoked by 10 mM Ca^{2+}, led to the release of weakly but electrostatically bound As towards newly available/accessible, high affinity sites. The consistent yet modest (ca. 25%) decrease in As(III) and As(V) bioavailability in the presence of Ca^{2+} (**Fig. 2**), supports the low number of strong As sites proposed by other studies (*21, 29*). Unfortunately, we do not yet have spectroscopic evidence supporting a change in bioavailability induced by conformational changes of DOM under our experimental conditions.

Finally, we performed a redundancy analysis (RDA) that assigns predictor variables to bioavailability measurements to explore the broad relationships existing between As species bioavailability and the various experiments performed in this study (**Fig. 3**). This analysis highlights that the drivers of As(III) and As(V) bioavailability in the presence of DOM are likely different, underscoring the relevance of our approach of performing speciation using a biosensor. Here, most variability was driven by predictor variables that align with RDA1 axis (N, S and aliphatic content of DOM) and with As(III) bioavailability vector. The magnitude of As(III) bioavailability in the presence of DOM appears to be less dependent on the presence of cations than As(V).

Indeed, and despite low coverage of the RDA2 axis (6.7%), alignment of As (V) bioavailability vectors with cationic treatment groupings and predictor variables suggest a stronger cationic interference on As (V) bioavailability, best characterized by Q1 (carboxylic) and Q2 (phenolic) pools of binding sites.

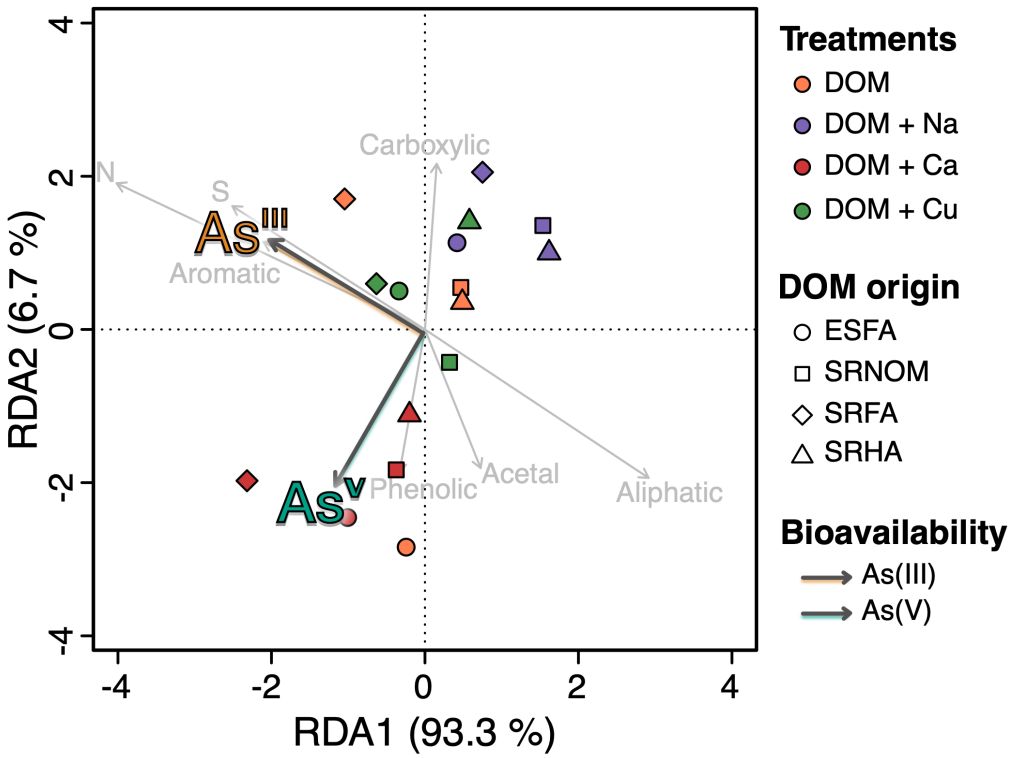

Fig. 3 | RDA triplot assigning predictor variables to drivers of bioavailability. Each RDA point represents ordination of biosensor outputs (**Fig. 2**) separated by Euclidian distances as a metric of variation. Overlaid are both bioavailability drivers (colored vectors) and explanatory variables (grey vectors), pointing in the direction of most rapid change. The angle between vectors of explanatory variables and bioavailability drivers reflect their linear correlation. Properties of the DOM origins used to produce this RDA can be found in Supplementary Information (**Supplementary Table**).

2.3. Arsenic photoreactivity and bioavailability in the presence of DOM

DOM can profoundly affect As(III) behavior in the environment. Here, DOM can compete with mineral adsorption sites, and enhance mobility of this contaminant by maintaining As in dissolved or colloidal forms (*53*). One important variable controlling the fate of DOM in natural surface waters is its photochemical reactivity which has also been involved in As redox transformations (*13, 54*). Moreover, the effects of As-DOM photoirradiation on As bioavailability have yet to be characterized. Such

information is relevant for situations when: i) groundwater reaches surface waters, ii) ice cover melts, iii) summer anoxia in DOM-rich wetlands/bogs, or iv) episodic draining and flooding of rice paddy soils. In this last series of experiments, we tested the role of As (III)-DOM photoreactivity on the bioavailability of As species (**Fig. 4**).

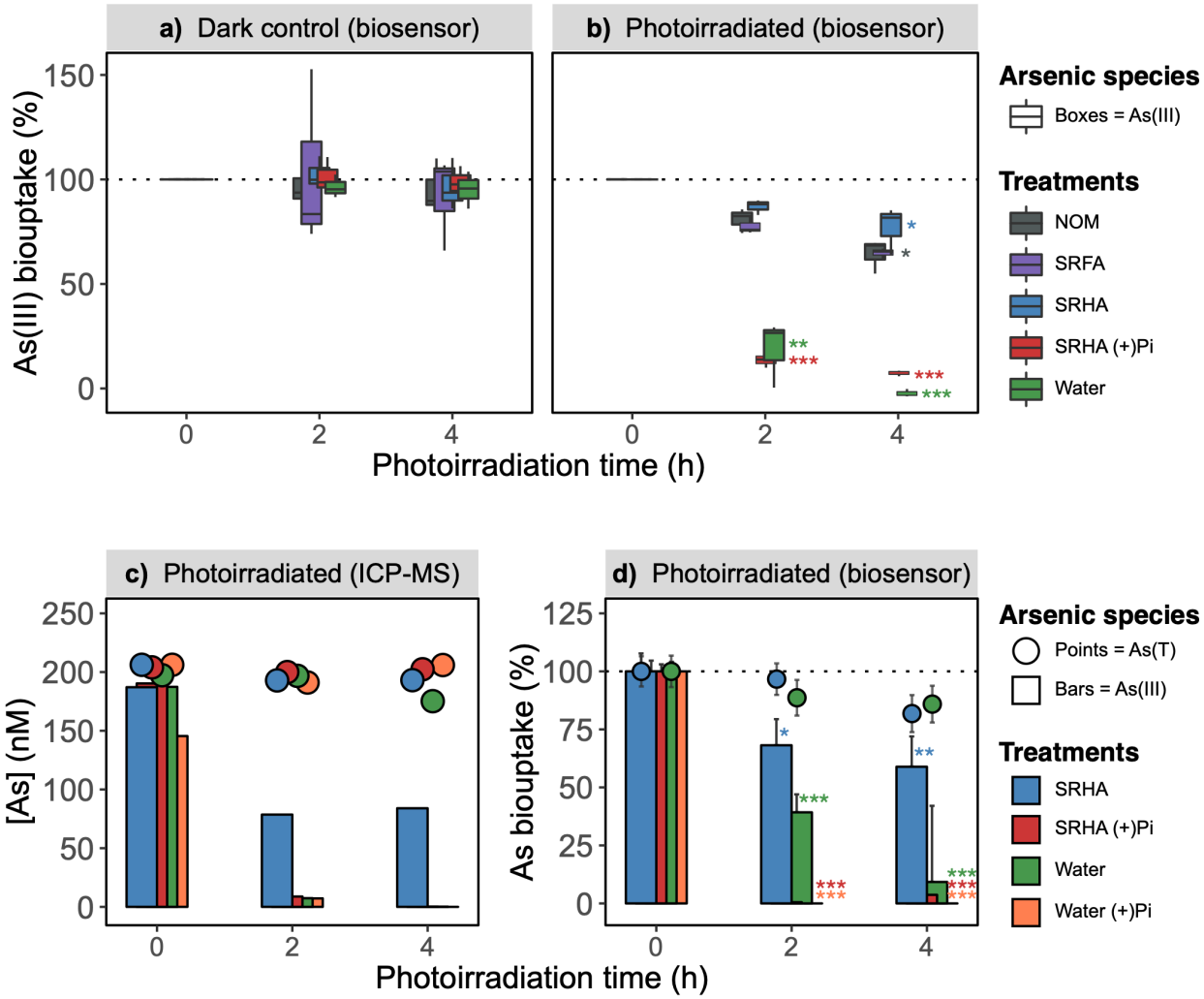

Fig. 4 | DOM affects the extent of As(III) photooxidation. HPLC-ICP-MS mass balance c) was used for validation of biosensor speciation technique a), b) and d) where a decrease in As(III) uptake over time suggests As(III) oxidation. Biosensor fluorescence was converted to percent biouptake (Y-axis) by comparing output signal of the irradiated treatments to the pre-irradiated (T0) controls. Biosensor endpoints present the mean and standard deviation of three independent biological triplicates. Panels b) and c) present an independent same-day mass balance using ICP-MS and biosensor outputs respectively. Dotted line represents biosensor output signal at T0. A significance code of (*) represents a p-value between 0.01 and 0.05 and of (***) for a p-value >0.001. Analysis of photoreactor light spectrum (**Fig. S5**) including supplemental controls for this figure, can be found in supplementary information (**Fig. S6**).

Our 2-step experimental treatment required the pre-incubation of a As(III) solution under UV–vis radiations (with or without DOM), prior to exposure to the biosensor assay. Upon exposure, only As(III) can be detected because, as per our protocol, 10 mM PO_3^- is added to the bioassay medium to prevent As(V) uptake (*22*). We observed that virtually none of the As(III) remained bioavailable after 4 h of irradiation in the absence of DOM (**Fig. 4**bd). In this case, a decrease of As(III) bioavailability could be attributed to i) conditions that directly prevents the biouptake of As(III) or ii) its oxidation to As(V). Our same-day control experiments analyzed using ICP-MS, confirmed the virtually complete As(III) oxidation to As(V) (**Fig. 4**c).

To maintain environmental relevance, no UVC bulbs were installed in our photoreactor. Yet in the absence of DOM and in the presence of light, oxidation of As(III) to As(V) in water alone was consistently observed in over two dozen separate replicated experiments. We performed a series of control experiments, to reasonably rule out the role of atmospheric gases (e.g. N_2, O_2, CO_2), the acid from the As stock solution preservative (HNO_3), and the nature of the cuvette container as sources and/or acceptors of electrons in the As(III) photooxidation process (**Fig. S6**, **Supplementary Method**). We sought to investigate whether water could be a source of HO• and H• radicals likely involved in As(III) photooxidation. Our spectroradiometer measurements confirmed that mostly visible spectral components (**Fig. S5**a) were emitted in the reactor with little spectral irradiance (0.166 $J•m^{-2}•s^{-1}$) in the UV regions (**Fig. S5**b). The photooxidation of As(III) at environmentally relevant levels (nM) requires only a relatively small number of photons emitted at water's ionization energy threshold (~6.5 eV) (*55*). In our incubation experiments, what appears as inconsequential spectral peaks (**Fig. S5**e) in the UV range (~6.1 eV), may provide the energy required to produce hydroxyl radicals needed to catalyze this reaction at the low As levels used. We unfortunately cannot properly report quantum efficiency yields considering CCD spectrometers sensors provide inaccurate

absolute intensity measurements due to the nature of their integrated analog (photons) to digital (volts) conversion process.

Surprisingly, the presence of DOM, amended as NOM, SRFA or SRHA greatly limited the extent to which As(III) was photooxidized to As(V) (**Fig. 4**). Hydroxyl radicals, regardless of their origins (water or DOM), can affect C-H and S-H bonds (*56*). This photochemical-induced conformational change of DOM could enhance binding of As-DOM. In either case, we suspected that the presence of DOM both attenuated photon flux via shading and limited As(III) photoreactivity via As-DOM binding.

Finally, we tested the role of a possible association between As(III) and DOM on As(III) photooxidation by adding phosphate to an As(III)-DOM solution prior to its photoirradiation. Our prediction was that addition of PO_4^{3-}, which is known to limit As(III) binding to DOM (*57*), would favour As(III) photooxidation by increasing the pool of unbound As(III) in solution. Indeed, in the presence of DOM + PO_4^{3-}, ICP-MS measurements indicated rates of As(III) photooxidation, similar to those observed in water alone. Our finding only partially supports previous literature claiming that As(III) oxidation is mediated by the transfer of electron from DOM (*13*). We cautiously conclude that differences among published results on the role of DOM on As photooxidation likely result from variable As-DOM binding conditions due to variation in Pi content (e.g., buffer), pH, and ionic strength of the exposure solutions. Overall, further experiments are required to determine the nature of the interaction between As and DOM in the presence of PO_4^{3-}. That being said, our data support our hypothesis that the nature and strength of As binding to DOM controls As bioavailability and reactivity.

3. CONCLUSION

It is generally accepted and often implied that the bioavailable fraction of As is the "free" or unbound one (*58, 59*). The work presented here showed that the bioavailable fraction of As is comprised of both labile and weakly complexed to DOM fractions. Though we found that 20 nmol As•mg^{-1} DOM ratio appears sufficient to saturate the low number of strong As binding sites in several types of commercially available DOM, further work is warranted to characterize the nature of weak vs strong As binding sites. Characterizing the strength and specificity of As-DOM interaction is fundamental in improving our understanding of microbially driven mobilization of As. This is an important gap of knowledge, which once addressed, will improve effective management of As contamination. Indeed, environmental changes brought by climate change such as variations in temperatures and precipitations already affect the physicochemical properties of natural waters making large-scale predictions on the fate of As-DOM complexes difficult (*11*). In the context of global water quality assessment, our work emphasizes the importance of considering the effects of climate change and of agricultural practices as they affect the levels of nutrients and their remobilization. Changes in DOM concentrations and nutrient levels may affect the fraction of As bound to DOM, which also control the bioavailability of As to the microbes responsible for its transformation and mobilization. Most importantly, this work calls for additional investigations on the kinetic controls that DOM exerts on As toxicity at various levels in food webs.

Acknowledgements

We would like to thank Dr. Emmanuel Yumvihoze for providing arsenic speciation analysis using HPLC-ICP-MS and Eric Kitchen for providing the spectroradiometer. This work was funded by an NSERC discovery grant, an Early Researcher Award from the Province of Ontario, and an NSERC Accelerator Grant funding to AJP, as well as Mitacs Globalink Research Award funding to MP, AJP, VL and BM.

Author contributions

MPP, AJP, VL, BM initiated and designed the experiments; MPP, VL, and CR carried out the experiments; MPP wrote the R scripts for data analyses; MPP wrote the manuscript with support from AJP, VL, BM, and CR; AJP, VL, and BM supervised the project. All authors have given approval to the final version of the manuscript.

Appendix A. Supplementary Information

Biosensor culture yield, fluorescence spectrum/intensity, bound vs bioavailable arsenic, photoreactor light spectrum, additional control experiments, and chemical properties of DOM extracts.

Abbreviations

As(III), arsenite; As(V), arsenate; DOM, dissolved organic matter; ESFA, Elliott Soil Fulvic Acid; HDPE, high density polyethylene; HPLC, high performance liquid chromatography; ICP-MS, inductively coupled mass spectroscopy; MGP, Mops Glycerophosphate; MIP, Mops Inorganic Phosphate; NOM, Natural Organic Matter; NSERC, Natural Sciences and Engineering Research Council of Canada; pMP01, Arsenic biosensor; RDA, redundancy analysis; SRFA, Suwannee River Fulvic Acid; SRHA, Suwannee River Humic Acid.

Declaration of interest statement

Authors declare no competing financial interest.

4. REFERENCES

1. I. W. G. o. t. E. o. C. R. t. Humans, W. H. Organization, I. A. f. R. o. Cancer, *Some drinking-water disinfectants and contaminants, including arsenic*. (IARC, 2004), vol. 84.
2. P. Ravenscroft, H. Brammer, K. Richards, *Arsenic pollution: a global synthesis*. (John Wiley & Sons, 2009), vol. 28.
3. C. E. Schuh, H. E. Jamieson, M. J. Palmer, A. J. Martin, J. M. Blais, Controls governing the spatial distribution of sediment arsenic concentrations and solid-phase speciation in a lake impacted by legacy mining pollution. *Science of the Total Environment* **654**, 563-575 (2018).
4. Y.-G. Zhu, X.-M. Xue, A. Kappler, B. P. Rosen, A. A. Meharg, Linking genes to microbial biogeochemical cycling: lessons from arsenic. *Environmental Science & Technology*, (2017).
5. J. Zhao *et al*., Diversity change of microbial communities responding to zinc and arsenic pollution in a river of northeastern China. *Journal of Zhejiang University-SCIENCE B* **15**, 670-680 (2014).
6. P. N. Bertin *et al*., Metabolic diversity among main microorganisms inside an arsenic-rich ecosystem revealed by meta-and proteo-genomics. *The ISME journal* **5**, 1735 (2011).
7. M. Grafe, M. Eick, P. Grossl, Adsorption of arsenate (V) and arsenite (III) on goethite in the presence and absence of dissolved organic carbon. *Soil Science Society of America Journal* **65**, 1680-1687 (2001).
8. E. Revesz, D. Fortin, D. Paktunc, Reductive dissolution of arsenical ferrihydrite by bacteria. *Applied Geochemistry* **66**, 129-139 (2016).
9. G. R. Willsky, M. H. Malamy, Effect of arsenate on inorganic phosphate transport in Escherichia coli. *Journal of Bacteriology* **144**, 366-374 (1980).
10. P. A. Riveros, J. E. Dutrizac, P. Spencer, Arsenic disposal practices in the metallurgical industry. *Canadian Metallurgical Quarterly* **40**, 395-420 (2001).
11. C. E. Williamson *et al*., Solar ultraviolet radiation in a changing climate. *Nature Climate Change* **4**, 434 (2014).
12. P. Langner, C. Mikutta, R. Kretzschmar, Arsenic sequestration by organic sulphur in peat. *Nature Geoscience* **5**, 66-73 (2012).
13. J. Buschmann, S. Canonica, U. Lindauer, S. J. Hug, L. Sigg, Photoirradiation of dissolved humic acid induces arsenic(III) oxidation. *Environmental Science & Technology* **39**, 9541-9546 (2005).
14. V. Lenoble *et al*., Evaluation and modelling of dissolved organic matter reactivity toward AsIII and AsV - Implication in environmental arsenic speciation. *Talanta* **134**, 530-537 (2015).
15. K. Kalbitz, R. Wennrich, Mobilization of heavy metals and arsenic in polluted wetland soils and its dependence on dissolved organic matter. *Science of the Total Environment* **209**, 27-39 (1998).

16. J. Buschmann *et al*., Contamination of drinking water resources in the Mekong delta floodplains: Arsenic and other trace metals pose serious health risks to population. *Environment International* **34**, 756-764 (2008).
17. S. H. Lamm, M. B. Kruse, Arsenic ingestion and bladder cancer mortality—what do the dose-response relationships suggest about mechanism? *Human and Ecological Risk Assessment* **11**, 433-450 (2005).
18. S. Dobran, G. J. Zagury, Arsenic speciation and mobilization in CCA-contaminated soils: Influence of organic matter content. *Science of the total environment* **364**, 239-250 (2006).
19. C. E. Williamson *et al*., Ecological consequences of long-term browning in lakes. *Scientific reports* **5**, 18666 (2015).
20. P. Thanabalasingam, W. Pickering, Arsenic sorption by humic acids. *Environmental Pollution Series B, Chemical and Physical* **12**, 233-246 (1986).
21. J. Buschmann *et al*., Arsenite and arsenate binding to dissolved humic acids: Influence of pH, type of humic acid, and aluminum. *Environmental science & technology* **40**, 6015-6020 (2006).
22. M. P. Pothier, A. J. Hinz, A. J. Poulain, Insights Into Arsenite and Arsenate Uptake Pathways Using a Whole Cell Biosensor. *Frontiers in Microbiology* **9**, (2018).
23. S. J. Driver, E. M. Perdue, *Advances in the Physicochemical Characterization of Dissolved Organic Matter: Impact on Natural and Engineered Systems*. F. Rosario-Ortiz, Ed., (2014), vol. Volume 1160.
24. J. D. Ritchie, E. M. Perdue, Proton-binding study of standard and reference fulvic acids, humic acids, and natural organic matter. *Geochimica et Cosmochimica Acta* **67**, 85-96 (2003).
25. IHSS. (International Humic Substances Society).
26. J. Stocker *et al*., Development of a set of simple bacterial biosensors for quantitative and rapid measurements of arsenite and arsenate in potable water. *Environmental Science and Technology* **37**, 4743-4750 (2003).
27. *Guidelines for drinking-water quality: recommendations* (9241546387, 2004).
28. K. Kalbitz, S. Solinger, J.-H. Park, B. Michalzik, E. Matzner, Controls on the dynamics of dissolved organic matter in soils: a review. *Soil science* **165**, 277-304 (2000).
29. G. Liu, Y. Cai, Complexation of arsenite with dissolved organic matter: conditional distribution coefficients and apparent stability constants. *Chemosphere* **81**, 890-896 (2010).
30. M. Vera *et al*., Fluorescence spectroscopy and parallel factor analysis as a dissolved organic monitoring tool to assess treatment performance in drinking water trains. *Science of the total environment* **584**, 1212-1220 (2017).

31. E. M. Murphy, J. M. Zachara, S. C. Smith, J. L. Phillips, T. W. Wietsma, Interaction of hydrophobic organic compounds with mineral-bound humic substances. *Environmental science & technology* **28**, 1291-1299 (1994).
32. D. Reynolds, S. Ahmad, The effect of metal ions on the fluorescence of sewage wastewater. *Water Research* **29**, 2214-2216 (1995).
33. I. Rathnayake, M. Megharaj, G. Krishnamurti, N. S. Bolan, R. Naidu, Heavy metal toxicity to bacteria–Are the existing growth media accurate enough to determine heavy metal toxicity? *Chemosphere* **90**, 1195-1200 (2013).
34. E. D. Amato *et al*., Assessing the effects of bioturbation on metal bioavailability in contaminated sediments by diffusive gradients in thin films (DGT). *Environmental science & technology* **50**, 3055-3064 (2016).
35. R. M. Amon, R. Benner, Bacterial utilization of different size classes of dissolved organic matter. *Limnology and Oceanography* **41**, 41-51 (1996).
36. J. B. McKinlay, J. G. Zeikus, Extracellular iron reduction is mediated in part by neutral red and hydrogenase in Escherichia coli. *Appl. Environ. Microbiol.* **70**, 3467-3474 (2004).
37. J. T. Nurmi, P. G. Tratnyek, Electrochemical properties of natural organic matter (NOM), fractions of NOM, and model biogeochemical electron shuttles. *Environmental science & technology* **36**, 617-624 (2002).
38. D.-Y. Huang *et al*., Comparison of dissolved organic matter from sewage sludge and sludge compost as electron shuttles for enhancing Fe (III) bioreduction. *Journal of soils and sediments* **10**, 722-729 (2010).
39. M. Miethke, M. A. Marahiel, Siderophore-based iron acquisition and pathogen control. *Microbiol. Mol. Biol. Rev.* **71**, 413-451 (2007).
40. E. Illés, E. Tombácz, The role of variable surface charge and surface complexation in the adsorption of humic acid on magnetite. *Colloids and Surfaces A: Physicochemical and Engineering Aspects* **230**, 99-109 (2003).
41. A. D. Redman, D. L. Macalady, D. Ahmann, Natural organic matter affects arsenic speciation and sorption onto hematite. *Environmental science & technology* **36**, 2889-2896 (2002).
42. E. Iskrenova-Tchoukova, A. G. Kalinichev, R. J. Kirkpatrick, Metal cation complexation with natural organic matter in aqueous solutions: molecular dynamics simulations and potentials of mean force. *Langmuir* **26**, 15909-15919 (2010).
43. Y. K. Mouvenchery, J. Kučerík, D. Diehl, G. E. Schaumann, Cation-mediated cross-linking in natural organic matter: a review. *Reviews in Environmental Science and Bio/technology* **11**, 41-54 (2012).

44. I. Christl, Magnesium binding by terrestrial humic acids. *Environmental Chemistry* **15**, 317-324 (2018).
45. A. A. Bonapasta, F. Buda, P. Colombet, G. Guerrini, Cross-linking of poly (vinyl alcohol) chains by Ca ions in macro-defect-free cements. *Chemistry of materials* **14**, 1016-1022 (2002).
46. I. Christl, Ionic strength-and pH-dependence of calcium binding by terrestrial humic acids. *Environmental chemistry* **9**, 89-96 (2012).
47. J.-P. Croué, M. Benedetti, D. Violleau, J. Leenheer, Characterization and copper binding of humic and nonhumic organic matter isolated from the South Platte River: evidence for the presence of nitrogenous binding site. *Environmental Science & Technology* **37**, 328-336 (2003).
48. D. Gondar *et al*., Copper binding by peat fulvic and humic acids extracted from two horizons of an ombrotrophic peat bog. *Chemosphere* **63**, 82-88 (2006).
49. E. Tipping, *Cation binding by humic substances*. (Cambridge University Press, 2002), vol. 12.
50. R. Sutton, G. Sposito, M. S. Diallo, H. R. Schulten, Molecular simulation of a model of dissolved organic matter. *Environmental Toxicology and Chemistry: An International Journal* **24**, 1902-1911 (2005).
51. W.-Y. Ahn, A. G. Kalinichev, M. M. Clark, Effects of background cations on the fouling of polyethersulfone membranes by natural organic matter: Experimental and molecular modeling study. *Journal of membrane science* **309**, 128-140 (2008).
52. A. Kalinichev, R. Kirkpatrick, Molecular dynamics simulation of cationic complexation with natural organic matter. *European Journal of Soil Science* **58**, 909-917 (2007).
53. G. Liu, A. Fernandez, Y. Cai, Complexation of arsenite with humic acid in the presence of ferric iron. *Environmental science & technology* **45**, 3210-3216 (2011).
54. S.-H. Yoon, J. H. Lee, S. Oh, J. E. Yang, Photochemical oxidation of As (III) by vacuum-UV lamp irradiation. *Water research* **42**, 3455-3463 (2008).
55. C. G. Elles, I. A. Shkrob, R. A. Crowell, S. E. Bradforth, Excited state dynamics of liquid water: Insight from the dissociation reaction following two-photon excitation. *The Journal of chemical physics* **126**, 164503 (2007).
56. G. V. Buxton, C. L. Greenstock, W. P. Helman, A. B. Ross, Critical review of rate constants for reactions of hydrated electrons, hydrogen atoms and hydroxyl radicals (· OH/· O– in aqueous solution. *Journal of physical and chemical reference data* **17**, 513-886 (1988).
57. S. E. Johnston, W. M. Barnard, Comparative Effectiveness of Fourteen Solutions for Extracting Arsenic from Four Western New York Soils 1. *Soil Science Society of America Journal* **43**, 304-308 (1979).

58. W. Sunda, Massachusetts Institute of Technology and Woods Hole Oceanographic Institution, (1975).
59. F. M. Morel, J. G. Hering, *Principles and applications of aquatic chemistry*. (John Wiley & Sons, 1993).

484